Evaluation of the applicability of nano-biocide treatments on limestones used in Cultural Heritage

Javier Becerra[1], Maripaz Mateo[2], Pilar Ortiz[1], Ginés Nicolás[2], Ana Paula Zaderenko[1]

[1]Departamento de Sistemas Físicos, Químicos y Naturales, Universidad Pablo de Olavide, Ctra. Utrera Km. 1, ES-41013, Seville, Spain

[2]Departamento de Ingeniería Industrial II, laser Applications laboratory, Universidade da Coruña, C/ Mendizabal s/n, ES-15403 Ferrol, Spain

Abstract

One of the main problems in the conservation of historical buildings and archaeological sites is the one caused by biodeterioration. Biopatina, biocrust or biofouling generate aesthetical changes and induce a degradation process within the stone matrix. In this work, three nanocomposites have been studied as potential biocides for limestones. These biocidal treatments are based on silver and silver/titanium dioxide nanoparticles synthesized following a bottom-up method with sodium borohydride as reducing agent. Nanocomposites have been characterized by UV-Visible spectrophotometry, Dynamic Light Scattering and Raman spectroscopy. These treatments were applied on limestones from three different Spanish quarries located in Utrera (Seville), El Puerto de Santa María (Cadiz) and Novelda (Alicante). The aesthetical modification of limestone surfaces was studied by colorimetric techniques and the effectiveness of protection against biofouling formation was tested using an accelerated biofouling growth assay. The best results were obtained for the treatments based on silver nanoparticles stabilized with citrate. The effectiveness of the treatments also depends on their penetration depth in the stone matrix and in this study, we have used Laser Induced Breakdown Spectroscopy to determine the depth profiles of nanocomposite presence in the stone matrix. Our results demonstrate that nanocomposites based on citrate-stabilized silver nanoparticles can be useful for the treatment of historical buildings and archaeological sites made of limestone, without producing high colour increments. Additionally, we have demonstrated the suitability of Laser Induced Breakdown Spectroscopy for the detection of silver/TiO_2 nanocomposites and for the generation of depth profiles.

Keywords

Biocide, colourimetry, cultural heritage, LIBS, limestone, silver/titanium nanocomposite

1. Introduction

One of the main problems in the conservation of historical buildings and archaeological sites is biodeterioration. The appearance of biofoulings, biopatinas or biocrusts generate aesthetical changes and degradation processes in the stone matrix. These altering agents have increased significantly over the last century due to factors such as high pollution levels [1]. Contributions from emerging disciplines, such as nanotechnology [2], is allowing for the design of new protective treatments. In this sense, the use of metal nanoparticles exhibiting bactericidal and biocidal properties to inhibit the biodegradation of stone monuments is noteworthy [3–7].

Silver nanoparticles are one of the most effective metal nanoparticles for use as microbiocides [8–10], and are widely employed in different fields such as medicine, cosmetics, textile industry or environmental remediation [11]. Titanium dioxide (TiO_2) nanoparticles on the other side are one of the most used nanoparticles due to their high versatility, especially as photocatalytic material [5,12] and also as biocide**s** [13,14]. The properties of these nanomaterials have been improved through the generation of nanocomposites, in which the interaction between silver and TiO_2 nanoparticles allows to enhance the properties of each nanomaterial separately [15]. In this case, the bactericidal capacity of silver nanoparticles is enhanced by the photocatalytic properties of the titanium dioxide nanoparticles [16,17].

The application of new treatments for conservation and restoration requires an exhaustive research on the performance and impact of these treatments on the stone matrix. This research must focus on guaranteeing their effectiveness as well as their applicability without changing the intrinsic aesthetical characteristics of the material in its pristine state.

In a previous work, nanocomposites based on titanium dioxide and/or silver nanoparticles were synthesized and tested for their capability to prevent biodeterioration of limestone extracted from a quarry in Utrera (South West Spain) and employed in historical monuments in Seville (Spain) [15]. Silver and titanium dioxide nanocomposites stabilized by citrate achieved a high biocide effect with low colour alteration.

2. Research aims

The aim of this research was twofold: On one hand, to probe the suitability of different nanocomposites based on silver and titanium dioxide as biocide treatments for historical buildings consisting of different limestone matrices. The aspects we focus on to evaluate the treatments are the aesthetical impact of the treatments and their biocidal activity compared with that of a biocide treatment widely used in restoration processes, Biotin T®. On the other hand, we also apply for the first time Laser Induced Breakdown Spectroscopy (LIBS) to this type of stone to evaluate the effectiveness of the treatments through their penetration depth profiles, and to determine the depth of nanocomposite presence in the stone matrices.

Laser Induced Breakdown Spectroscopy (LIBS) is a minimally invasive technique which does not require sampling and allows in situ analysis [18,19], that has been used to determine the material composition [20–26] or stratigraphic sequence of artworks [27]. These characteristics make LIBS the ideal technique to achieve this purpose, compared with techniques such as scanning electron microscopy coupled to an X-ray dispersive energy detector (SEM-EDX) [28,29].

3. Materials and Methods

3.1. Synthesis and characterization of treatments

Three treatments based on silver and titanium dioxide nanoparticles have been studied as biocides for historical and contemporary buildings. Two different syntheses were employed. The main difference between them is whether or not trisodium citrate is used as stabilizing agent. Silver/titanium dioxide nanocomposites (Ag/TiO_2) were prepared by reduction of silver nitrate ($AgNO_3$) with sodium borohydride ($NaBH_4$) in aqueous solution [15]. Briefly, 4 mL of an aqueous solution of $NaBH_4$ (0.01 mmol) were added to 20 mL of an aqueous solution of $AgNO_3$ (1mM) and TiO_2 (10 mg)) under magnetic stirring in an ice bath. The reaction mixture was stirred for 10 min. The suspension obtained was kept in the dark until its application on stone samples. Citrate-capped silver nanoparticles (AgCit) were synthesized by reduction of $AgNO_3$ with $NaBH_4$ in an aqueous solution and stabilized by trisodium citrate [15]. Briefly, 1 mL of an aqueous solution of $AgNO_3$ (5 mM) was added to 16 mL of an aqueous solution of trisodium citrate (1.06 mM) under magnetic stirring in an ice bath. Then, 100 µL of an aqueous solution of $NaBH_4$ (100 mM) were added dropwise and the final solution was stirred for 105 min. The resulting suspension was kept in the dark until its use on stone samples. Citrate-capped silver /titanium dioxide

nanocomposites (AgCit/TiO_2) were prepared as described above but adding 9.6 mg of TiO_2 nanoparticles to the initial 16 mL of aqueous solution containing trisodium citrate.

Silver nitrate ($AgNO_3$) and trisodium citrate were purchased from Panreac, titanium dioxide (P25) from DEGUSSA and sodium borohydride ($NaBH_4$) from Sigma-Aldrich. All other chemicals were reagent grade. Water was purified using a Milli-Q reagent grade water system from Millipore.

All nanocomposites were characterized by UV-Visible (UV-Vis) spectrophotometry, Dynamic Light Scattering (DLS) and Raman spectroscopy. UV-Vis spectra were recorded on an Ocean Optics spectrometer equipped with a HR4000 detector (Dunedin, FL. USA). Zeta potential (ζ) and hydrodynamic diameter (HD) were determined by DLS on a Zetatrac Analyzer (Microtrac, USA). Raman spectra were recorded on a Bruker Senterra confocal Raman microscope equipped with a laser excitation of 785 nm and a DU420A-OE-152 detector.

3.2. Aesthetical impact of the treatments over different limestones

One of the most common types of stones used as building materials in southern Spain since ancient times are limestones. This can be seen from the abundance of quarries of this porous carbonated stone. The assay of treatments was carried out on limestones from three origins, Utrera (Seville), Puerto de Santa María (Cádiz) and Novelda (Alicante). These quarries have been active and provided the building materials for many a historical and contemporary building in Spain [30–32]. Table 1 shows the main characteristics of these limestones according to the studies carried out by Guerrero [33] and the measure of the open porosity at atmospheric pressure carried out according to UNE-EN 13755:2008 [34]. The geographical location of the provinces of the quarries is depicted in Figure 1.

Table 1. Properties of limestones by quarry

Quarry	**Type**	**Pore diameter (μm)**	**Open porosity (%)**
El Puerto de Santa María (Cadiz)	calcarenite	10 – 100	17±3
Utrera (Seville)	biosparite	0.1 – 1.4	8±1
Novelda (Alicante)	biosparite	0.01 – 0.5	5±2

Fig. 1. Location of the provinces of the three quarries considered in this study on the map of Spain.

The size of slabs used in this study was 1.5 x 1.5 x 0.5 cm. Two applications of 200 mL of aqueous suspension of nanocomposites were deposited over each surface slabs, using equal concentration referred to silver (0.015 mg/mL) for each treatment (i.e. 0.015 mg/mL AgCit, 0.145 mg/mL AgCit/TiO_2 or 0.1 mg/mL Ag/TiO_2). The stones treated were dried at room temperature (24±2°C).

Treatments for conservation-restoration must avoid altering the aesthetical characteristics of the artworks on which they are applied. Surfaces of the stone slabs were analysed before and after application of treatments by colorimetry using a PCE-CSM 2 (diameter of circular measuring area: 8 mm, daylight illumination: D65). Colour measurements were carried out using the parameters defined by the CIELAB colour-system. Chromatic variations (ΔE^*) after treatments were calculated according to Eq.1

$$\Delta E^* = \sqrt{\Delta L^{*2} + \Delta a^{*2} + \Delta b^{*2}} \quad , \qquad \text{Eq.1}$$

where ΔL^*, Δa^* and Δb^* characterize variations of the colour values as referred to the control in the black-white (brightness), red-green and yellow-blue axes, respectively.

Due to the absence of standardized rules for the interpretation of colour changes in treatments on cultural heritage stones, the most common practice is to accept $\Delta E^*<5$ [35–37]. Nevertheless, some authors like García and Malaga [38] and Ortiz et al. [25] propose three ranges of chromatic changes for dyes in Cultural Heritage porous materials: $\Delta E^*<5$, chromatic changes cannot be detected by the human eye; $5<\Delta E^*<10$, chromatic changes can be detected by the human eye but are still acceptable; and $\Delta E^*>10$, chromatic changes are clearly visible.

3.3. Evaluation of the penetration of the AgCit/TiO_2 treatment by LIBS

The measurement of the nanoparticle penetration depth is of great relevance because the biocide effectiveness of the treatments depends on it. For this reason, in this work LIBS technique was tested for the in-depth characterization of the nanoparticle treatment. In particular, a preliminary penetration study by LIBS was carried out in Novelda limestone treated with AgCit/TiO_2. On the other hand, when we analysed the nanoparticles in the limestone stemming from El Puerto de Santa María, their spectral signal was so weak or instable in most of the analyses that reliable conclusions on penetration could not be extracted due to the high porosity of the sample (17±3%), and the size of the pores (10 – 100μm). For all these reasons, special attention was dedicated to Novelda limestone in this study.

In particular, this work focused on the AgCit/TiO_2 treatment due to its high biocidal effectiveness. The experimental setup employed for LIBS measurements consisted of a typical single pulse LIBS setup. In particular, the second harmonic wavelength (532 nm) of a Q-Switched Nd:YAG laser (Brilliant, Quantel, 5 ns pulse width) was used to perform the LIBS analyses at a laser-pulse energy of 27 mJ. The laser beam was focused at normal incidence onto the sample surface by a plano-convex quartz lens (f = 100 mm) to ablate the sample and generate a plasma whose radiation was guided by means of a quartz optical fiber to the entrance slit of an Echelle spectrograph (Mechelle, Andor). There, the plasma light was dispersed and detected by an ICCD camera (iStar, Andor). The spectral region comprised from 200 to 850 nm. For the emission spectra acquisition, temporal parameters of 2.5 μs and 10 μs were selected for time delay and integration time, respectively. All the LIBS measurements were performed in air under atmospheric pressure.

3.4. Accelerated biofouling growth test and biocidal effectiveness

Accelerated biofouling growth test was carried out by immersion of treated slabs inside a culture tank at room temperature (24±2^{o}C) and permanent lighting according to Becerra et al. [15]. For this study, a limestone from the Utrera quarry was selected. Its principal physical properties are described in Table 1. One dose of 200 μL of a water suspension of the nanocomposite at the final concentration of 0.03 mg/mL AgCit, 0.29 mg/mL AgCit/TiO_2 or 0.2 mg/mL Ag/TiO_2 were spread over the limestone surface with a plastic spatula. Additionally, these treatments were compared with one of the most common biocidal treatments used in cultural heritage, Biotin T®. This biocide was used following the commercial recommendation, spreading 200 μL of an

aqueous dissolution of the product at a 1% concentration. The stone slabs were dried at room temperature (24±2 °C) during 5 days before immersing the slide in the tank.

To design the accelerated biofouling growth test, we used real-life biofilm taken from the façades of thirteen churches of Seville (Spain). The samples of biofilm were cultured in a phosphate-rich medium ($NaH_2PO_4x2H_2O$, 20 mg/L) during 9 days at room temperature (24±2 °C) and exposed to solar light (14 hours per day). A preliminary identification carried out by optical microscopy (Leica DM2500 optical microscope) allowed us to identify the main chlorophyta (green algae): Chlorella sp., Botryococcus sp., Cyclotella sp., Monoraphidium sp. and Phytoflagellate sp. and the main cyanobacteria (blue-green algae): Gloeocapsa sp. and Nostoc sp.

The previously prepared algal culture was employed to perform an accelerated biofouling growth test at the concentration of 0.15 g/L. The treated slabs were immersed in the culture tank for 56 days. The surface slabs were analysed before and after assay by means of a handheld digital microscope (Zarbeco MiScope MP2) with 40-140X magnification lens. The suitability of the nanocomposites to inhibit the generation of biofouling was assayed by means of spectrophotometric colour measurements. This method is emerging as an improved alternative to previous methods such as fluorescein diacetate hydrolysis or chlorophyll α determination [39–42] due to its advantages such as it being a non-destructive technique that can be performed on-site and not requiring expensive and time-consuming sample preparation [40–42]. Chromatic changes (ΔE*) were calculated before (ΔE*[ab]) and after (ΔE*[pb]) accelerated biofouling growth test according to Eq. (1) where L*, Δa*and Δb* were calculated as the variations between initial and final colour slabs for every process of the assay: ΔE* caused by the treatments (ΔE*[ab]) and by the biofouling (ΔE*[pb]).

Additionally, the effectiveness of each treatment to inhibit the biofouling growth (ET) was calculated according to Eq.2

$$ET = \left| \frac{\Delta E^*[pw]_{\text{untreated sample}} - (\Delta E^*[pw])}{\Delta E^*[pw]_{\text{untreated sample}}} \times 100 \right| \qquad \text{Eq. (2)}$$

where ΔE*[pw] is the colour change caused by the biofouling growth over the limestone surfaces.

4. Results and discussion

4.1. Treatments of nanocomposites

Three biocidal treatments based on silver/titanium dioxide nanoparticles were synthesized. In order to confirm the outcome of the synthesis, Raman spectroscopy and UV/Vis spectroscopy were employed. Raman spectroscopy spectra (Fig. 2A) show the specific composition of each treatment. Although the metallic Ag cannot be detected by Raman spectroscopy [43], it is possible to detect it indirectly by its interaction with other elements. For example, AgCit nanoparticles showed a strong band at 240 cm^{-1} due to the stretching vibrations of Ag-O bonds [44,45]. The vibrational modes of Ti-O could be observed at 400, 520 and 640 cm^{-1} [46].

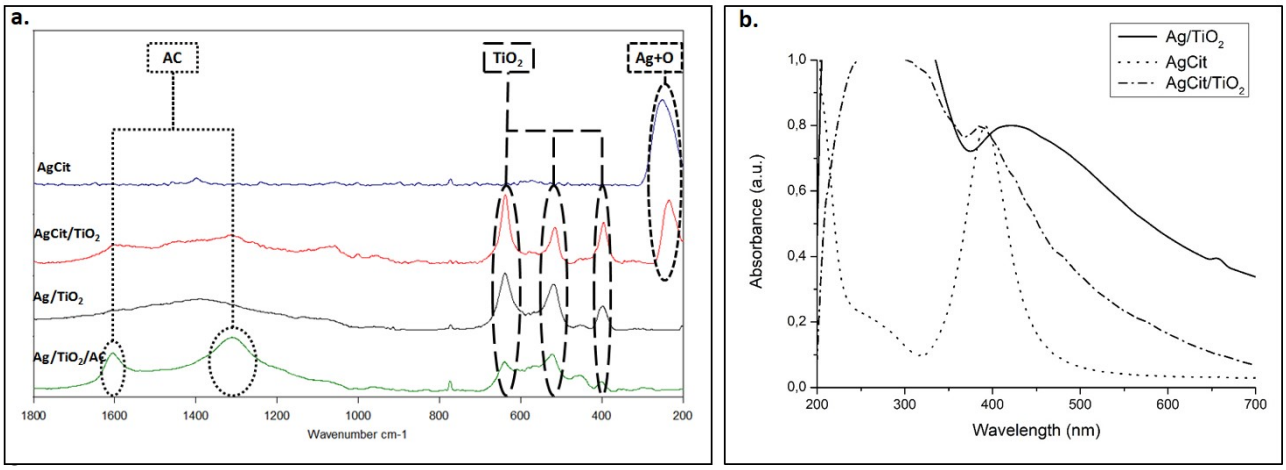

Fig. 2. Raman (A) and UV-Vis (B) spectra of the different nanocomposites.

Table 2 shows the hydrodynamic diameter (HD) and Zeta potential (ζ) of the aqueous dispersions of the different treatments. As expected, the lowest HD and highest ζ values were obtained for the citrate-capped silver nanoparticles (AgCit). It is important to highlight that the treatment based on silver and TiO_2 had a similar HD, although Ag/TiO_2 nanocomposite has a higher polydispersion. Furthermore, $AgCit/TiO_2$ had a higher ζ-potential due to the negative charge provided by the trisodium citrate. In this sense, the presence of trisodium citrate contributed to increase the colloidal stability to a value close to |30|mV, value generally acknowledged as the limit between stable and unstable colloids [47]. This was confirmed by UV-Vis spectroscopy, in which unstable nanoparticles show a noticeable broadening of the silver plasmon band and a shift towards higher wavelengths [48]. The bands of the naked-silver nanocomposite (Fig. 2B) had this increment throughout the visible region, evidencing their tendency to aggregate and a higher instability in aqueous suspension. Additionally, the wavelength of the maximum of the plasmon peak of the silver nanoparticles is related to their size; lower wavelengths are related to decreasing size [48]. AgCit and its TiO_2-derived nanocomposite displayed a smaller size of silver nanoparticles than the Ag/TiO_2 nanocomposites, with a plasmon peak at 390 nm.

Table 2. Hydrodynamic diameter (HD) and zeta potential (ζ) of the different types of treatments.

Treatment	HD (nm)	ζ (mV)
AgCit	36±8	-63±3
AgCit/TiO_2	72±18	-24.8±0.3
Ag/TiO_2	94±33	-17±3

4.2. Aesthetical impacts of the treatments on different limestones

The aesthetical impact of the treatments was measured by chromatic changes. Table 3 shows the chromatic coordinate increments ΔL*, Δa*and Δb* obtained for the different stone slabs. ΔE* was calculated to evaluate the applicability of these treatments on stone monuments without changing their chromatic properties.

The main effect of the treatments of the stone surface was a change in luminosity (L). ΔL was always negative causing darkening as can be seen in Fig. 3.

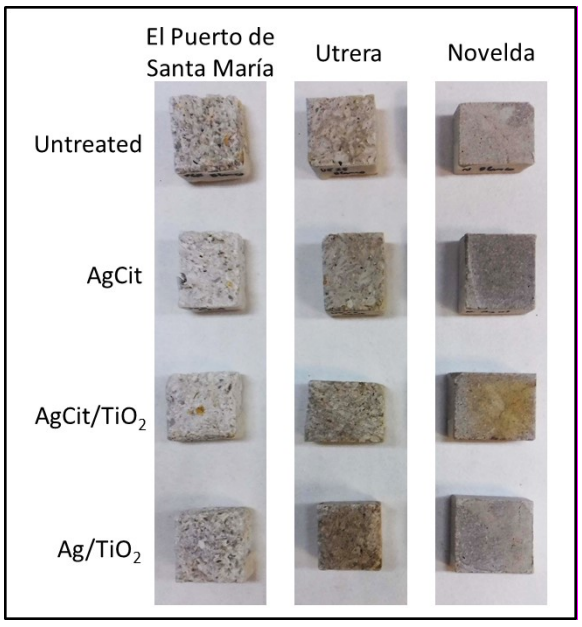

Fig.3. Digital photographs of limestone slabs after application of nanocomposites.

The chromatic changes for every treatment were dependent on the intrinsic characteristics of the stone matrices. As can be observed in Table 3, ΔE* was lower in the stone slabs from the quarry of El Puerto de Santa María (close to 1). This is due to the higher open porosity (17%) and

pore sizes (10-100 µm) of this limestone, characteristics that favour the easy penetration of the treatments into the stone matrix. As a consequence, the chromatic changes were more evident when the open porosity and the pore sizes decrease. Slabs from the quarry of Novelda showed a higher increment of ΔE*, although only in the case of AgCit/TiO_2 was it actually above 10, invalidating the treatment for this limestone.

Additionally, the own characteristics of each treatment had a strong influence on the final appearance of the stone surface. AgCit was the treatment that caused a lower ΔE* (between 0.9 and 5.7) due to its smaller HD (36 nm) and its higher ζ (-63 mV) that improves its penetration into the stone matrix. On the other hand, a higher HD together with a lower ζ favours their deposition on the stone surface and the formation of aggregates, causing higher increments of ΔE*. This could be due to the fact that the concentration of the aqueous suspension of all nanocomposites was adjusted to obtain 0.015 mg/mL referred to silver, so treatments that included significant titanium dioxide were in effect applied more concentrated (on a per mass basis) than the AgCit treatment (the citrate coating has only a marginal effect on total weight of the nanoparticles). Therefore, the excess of nanocomposites of these treatments precipitates on the stone surface causing an increment in the total colour change.

Table 3. Increases of colour caused by the application of nanocomposites. Initial colour is the colour after treatment, final colour after the accelerated weathering process. Error bars are due to natural variability of the samples.

Quarry	Treatment	Initial colour			Final colour			Colour increments			
		L	a*	b*	L	a*	b*	ΔL*	Δa*	Δb*	ΔE^*
Puerto de Sta. María (Cádiz)	*AgCit*	84±0.5	3±0.1	12±0.2	84±0.6	3±0.1	13±0.4	-0.61	0.11	0.71	0.94
	AgCit/TiO_2	84±0.4	3±0.2	13±0.1	83±0.2	3±0.2	14±0.6	-0.63	0.27	0.12	0.70
	Ag/TiO_2	85±0.2	3±0.1	11±0.1	84±0.2	3±0.1	11±0.1	-1.19	0.17	-0.07	1.20
Utrera (Sevilla)	*AgCit*	77±0.1	4±0.1	14±0.1	73±0.1	4±0.1	15±0.1	-4.28	0.35	1.45	4.53
	AgCit/TiO_2	76±0.7	3±0.2	14±0.1	73±0.3	5±0.1	17±0.4	-2.94	1.44	2.58	4.17
	Ag/TiO_2	78±0.3	4±0.1	14±0.1	73±0.1	6±0.1	17±0.1	-4.73	1.97	2.58	5.73
Novelda (Alicante)	*AgCit*	73±0.2	3±0.1	10±0.1	67±0.4	3±0.1	11±0.1	-5.57	0.43	1.09	5.69
	AgCit/TiO_2	76±0.5	3±0.1	11±0.3	70±0.2	6±0.1	22±0.2	-5.95	3.13	11.12	13.00
	Ag/TiO_2	71±0.1	4±0.1	11±0.1	65±0.1	7±0.1	15±0.3	-6.67	3.47	4.23	8.63

Finally, about the applicability of these treatments to Cultural Heritage, ΔE* is lower than 1 in the case of the most porous stones (El Puerto de Santa María). Only in the limestone with the lowest porosity (Novelda), the colour change was close to 10 and, as a consequence, it is advisable to lower the concentration employed to decrease the aesthetic impact.

4.3. Evaluation of the penetration of the AgCit/TiO_2 treatment by LIBS

The penetration of the biocide treatments based on nanoparticles is not usually measured. Nevertheless, the treatment effectiveness depends on the penetration of these nanomaterials. For this reason, LIBS technique was tested in this work for the in-depth characterization of the nanoparticles treatment in stones, in particular in Novelda limestone, as complementary studies related to the biocidal effectiveness. LIBS is an emission spectroscopy technique that employs a pulsed laser beam that is focused to ablate a tiny portion of the sample surface and to generate a plasma from the ablated material. The spectral analysis of the light emitted from that plasma provides information about the elemental composition of the sample at the analysed position. In addition, depth-resolved compositional information can be also obtained by LIBS. For that purpose, if the laser is fired repetitively over a single position of the sample surface, depth-related spectra can be obtained by monitoring laser-induced plasma emission from each laser shot. This procedure was followed in this work to obtain the depth-dependent distribution of the AgCit/TiO_2 following treatment of the Novelda limestone. The results for one analysis are shown in Fig. 4 in two ranges of wavelengths, around 338 nm (Fig. 4 top) and around 521 nm (Fig. 4 bottom). The in-depth sequence of emission spectra of Fig. 4 top and bottom corresponds to 50 and 10 in-depth laser pulses, respectively. As shown, the peaks corresponding to Ag (I) at 338.289 nm emission line (Fig. 4 top) and to Ti (I) 521.0384 nm (Fig. 4 bottom) can be identified in the spectra, demonstrating that the sensibility of the technique is good enough for this type of analysis. It should be noted that the correct identification of the peaks was corroborated by comparison with the spectra obtained from reference samples of silver and titanium. As shown in Fig. 4, the signals of Ag and Ti decay with the number of in-depth pulses, as expected, due to the diffusion of the nanoparticles inside the limestone matrix. In order to study with more detail the evolution of Ag and Ti signal with depth, the associated depth profiles were generated.

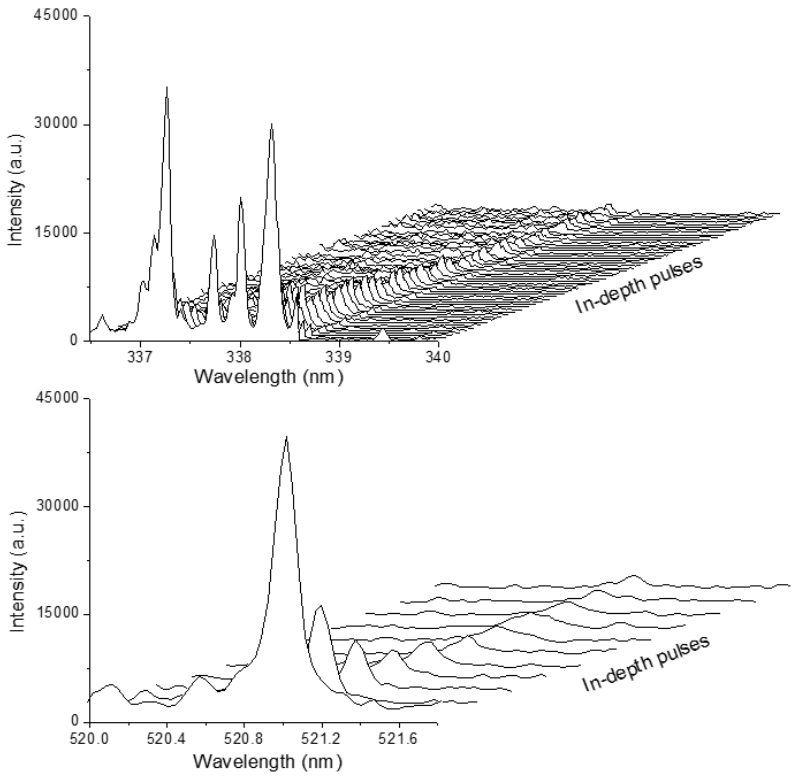

296

297 Fig. 4. In-depth sequence of LIBS spectra obtained from Novelda limestone treated with
298 AgCit/TiO_2 in two ranges of wavelengths.

299 Fig. 5 shows the depth profiles of Ag and Ti generated by plotting emission intensities against
300 the number of pulses at specific wavelengths, 338.289 nm and 521.0384 nm, for Ag and Ti,
301 respectively. As can be observed, both profiles exhibit a decaying trend until a certain number
302 of pulses, as the presence of nanoparticles decreases with depth. However, in the profiles of
303 Figure 5 corresponding to the same analysis, the Ti signal disappears faster with depth compared
304 to the Ag signal. In this sense, while the Ag signal stops decaying after about 33 pulses, the Ti
305 signal goes down during the first 10 pulses and then it is almost negligible. The explanation of
306 this effect is still under study and the possibility of the presence of different types of
307 nanoparticles with different penetrations after the treatment is being considered.
308 Unfortunately, the sensibility of scanning electron microscopy with X-ray dispersive energies
309 was not sufficient to detect the nanoparticles in the analyses realized with the aim of providing
310 additional information about the identity and diffusion of the nanoparticles. In order to achieve
311 an estimation of the penetration depth of the nanoparticles from the LIBS profiles, it is necessary
312 to get a depth scale to convert the number of pulses into depth. For that purpose, an ablation
313 rate of 6 µm/pulse was calculated by measuring, using optical microscopy, the depth of craters
314 generated by a different number of pulses in the analyzed sample. The calculated average
315 ablation rate was used to convert the number of in-depth laser pulses where the signal stops

decaying in the profiles of Fig. 5 into depth, resulting in estimated values of penetration of 198 µm, when Ag signal is considered, and of 60 µm when Ti signal is analyzed. These results demonstrate the potential of LIBS technique for the in-depth characterization of nanoparticle treatments in stones.

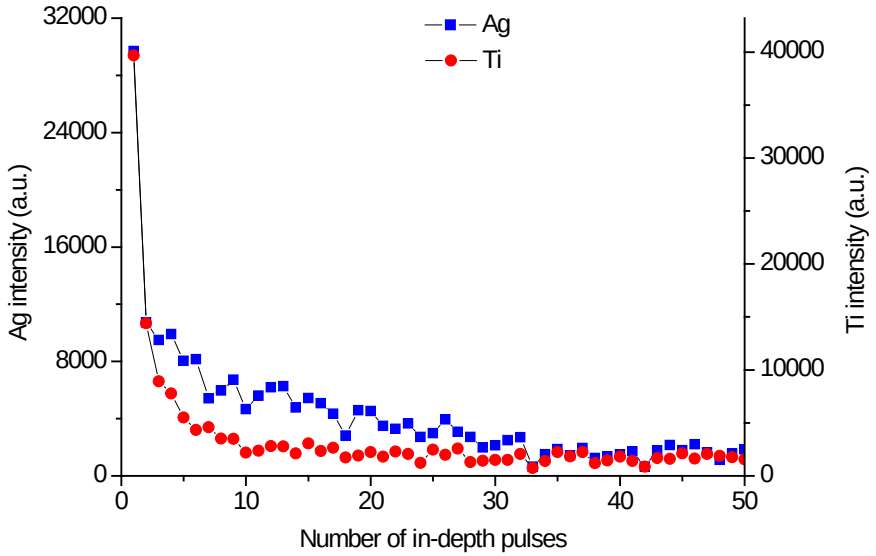

Fig. 5. Depth profiles of Ag (I) 338.289 nm (■)and Ti (I) 521.0384 nm (●) obtained from LIBS analysis of Novelda limestone treated with AgCit/TiO_2.

4.4. Accelerated biofouling growth test and biocidal effectiveness

The capability of the treatments based on silver/titanium nanocomposites to inhibit the generation of biofouling was assayed by means of colorimetric measurements. The increments of colour (ΔE*) in limestone slabs were calculated before (ΔE*[ab]) and after (ΔE*[pb]) the accelerated biofouling growth test. In this sense, the treatments did not cause any noticeable aesthetical change in the limestone slabs as can be seen in Fig. 6. Table 4 shows chromatic increments (ΔE*[ab]) close to 5 what validated the treatments for their application on similar limestones used in historical and contemporary buildings.

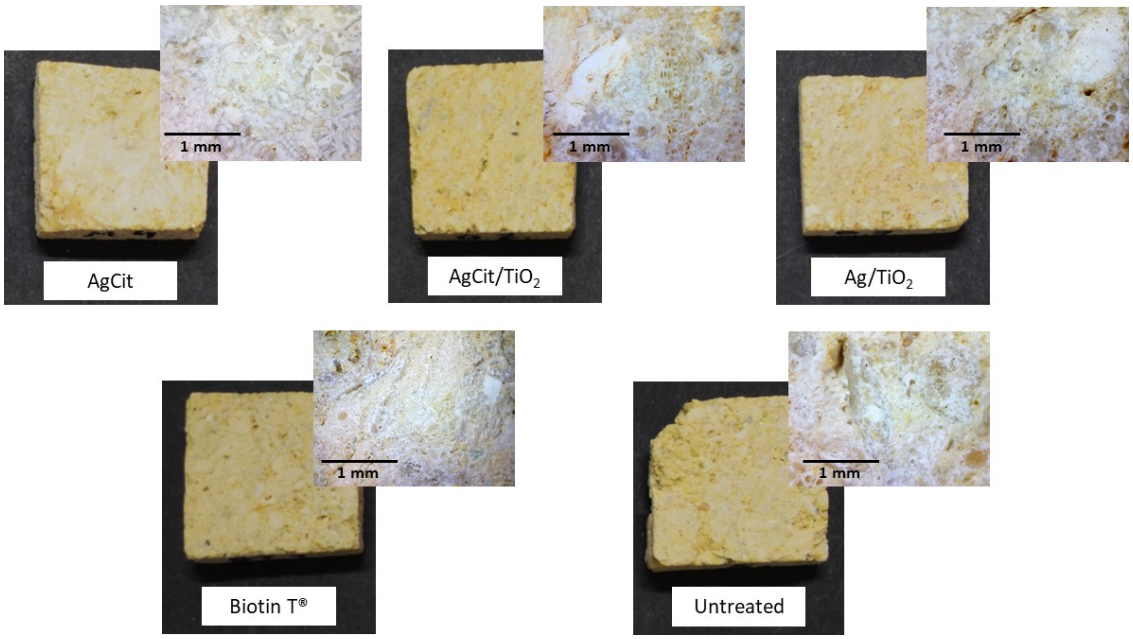

Fig. 6. Digital images of the limestone slabs after the treatment application and details captured by a handheld digital microscope at a magnification of 140x.

Table 4. Increases of colour caused by the application of nanocomposites and the generation of biopatina

	ante-biofouling test [ab]				post-biofouling test [pb]				Effectiveness
Product	**ΔL***	**Δa***	**Δb***	**ΔE***	**ΔL***	**Δa***	**Δb***	**ΔE***	***[ET] (%)***
AgCit	*-3.9±1.3*	*0.8±0.3*	*2.9±1.1*	*4.9±1.7*	*-0.3±1.3*	*1.2±0.8*	*2.2±2.7*	*3.5±1.4*	*74.4*
AgCit/TiO_2	-4.6±2.4	*1.2±0.5*	*3.2±2.0*	*6.0±2.4*	*-0.2±0.6*	*-2.5±0.3*	*-2.4±1.4*	*3.6±1.0*	*73.8*
Ag/TiO_2	*-4.0±1.6*	*1.0±0.5*	*2.8±1.5*	*5.0±2.1*	*-6.9±1.5*	*4.1±0.8*	*15.2±3.4*	*17.2±3.7*	*-25.3*
Biotin T	*-0.4±0.1*	*0.0±0.1*	*0.0±0.3*	*0.5±0.2*	*-2.9±1.2*	*0.5±0.5*	*5.6±1.3*	*6.4±1.8*	*53.4*
Untreated	-	-	-	-	*-6.9±1.2*	*0.9±1.1*	*11.8±2.8*	*13.7±3.0*	-

Remarkable differences were observed in the results related to their biocidal properties. In the case of the citrate-capped silver nanoparticles (AgCit and AgCit/TiO_2), the colour modification generated by the biofouling (ΔE*[pb]) were about 3.5 (Table 4). Isolated aggregates of algae were observable on the surface of the limestones treated with these products (Fig. 7). On the contrary, the use of the nanocomposite based on naked silver nanoparticles did not inhibit the biofouling formation, achieving a similar aesthetical damage than the untreated limestones. These results are in agreement with previous studies [15,49], although the effectiveness of the AgCit treatment has increased when the duration of the assay was doubled (from 28 to 56 days), confirming its suitability as preventive treatment.

The comparison between the new treatments based on nanocomposites and the widely employed Biotin T® showed that the citrate-capped silver nanoparticles were 20% more effective preventing the biofouling formation. This result is in agreement with Fonseca et al. [50], who conclude that nanoparticles (TiO_2) are better agents for preventing the biodeterioration than the conventional biocides such as Biotin T®.

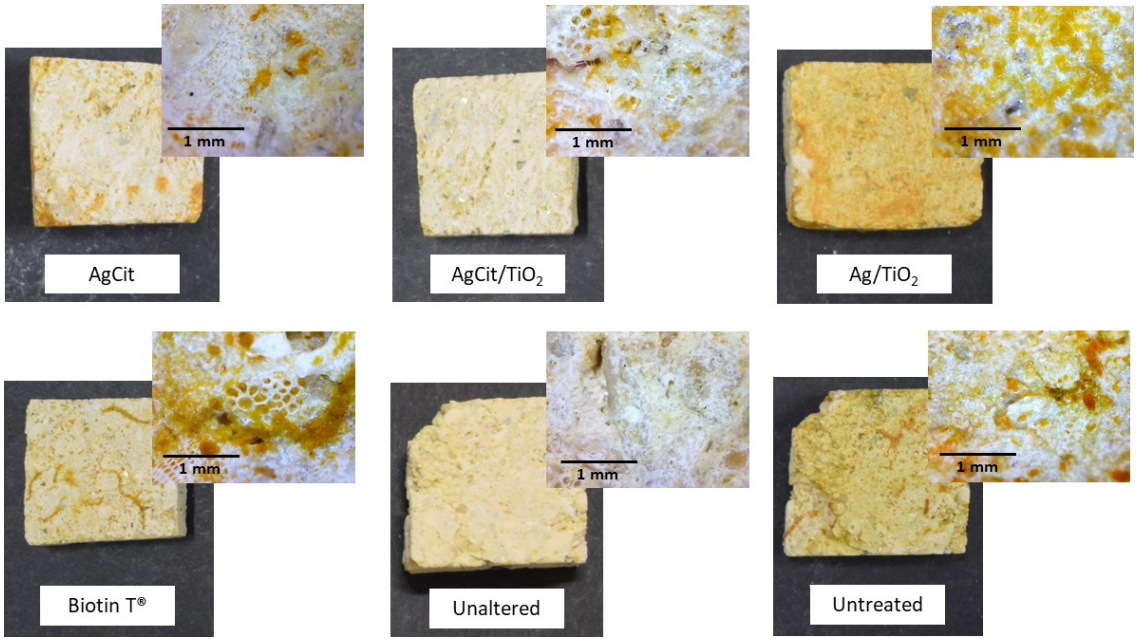

Fig. 7. Digital images of the limestones slabs after the accelerated biofouling growth test and details captured by a handheld digital microscope at a magnification of 140x. An example of unaltered limestone slabs was included as a comparison with the results achieved.

5. Conclusions

The design of treatment based on nanoparticles allows to achieve new products for the conservation and restoration of cultural heritage. In this research, new biocides based on silver/titanium nanoparticles were probed on limestone. To validate these treatment for cultural heritage, some requirements need to be met such as having little impact on aesthetical properties and a good effectiveness.

The main difference between the treatments is the use of trisodium citrate as stabilizing agent. The stabilization of the silver nanoparticles allows to decrease the hydrodynamic diameter and increase the stability of the colloidal dispersion. In this sense, AgCit nanoparticles showed the

best properties for its applications on limestones due to a hydrodynamic diameter lower than 40 nm and a zeta potential higher than 60 mV.

The aesthetical compatibility of the treatments was studied in different limestones used in historical and contemporary buildings. The best result was achieved with AgCit nanoparticles. This product caused colour increments close to 5 and, consequently, is appropriate for cultural heritage materials. The silver/titanium dioxide nanocomposites are compatible with the aesthetical values of limestones whose porosity is higher than 8% and has, at least, a pore diameter of 0.1 μm. However, when these treatments (AgCit/TiO_2 and Ag/TiO_2) were applied on limestones with a low porosity or porous size (Novelda), the colour increments are higher than expected. One solution in these cases could be to apply the product more diluted, avoiding the precipitation of the nanocomposite on the stone surface.

The treatments based on silver nanoparticles stabilized with citrate had a strong capability to inhibit the biofouling formation with respect to the untreated samples. This effectiveness is widely higher than the result achieved by Biotin T®, one of the most common biocides used in cultural heritage, that only reduced the biofouling formation by 53%.

In addition, the results obtained by LIBS for the in-depth characterization of the AgCit/TiO_2 treatment in Novelda limestone demonstrate the potential of the technique as a powerful tool to complete the effectiveness study of the biocidal treatments in terms of penetration depth and they establish the basis for new comparative studies.

In summary, the treatments based on citrate-capped silver nanoparticles (AgCit and AgCit/TiO_2) have been the most efficient preventing the appearance of biofouling in more than 70%. Nevertheless, the selection of one or the other depends on the physical properties of the substrate, although it is possible to decrease their aesthetical impact by reducing the concentration of the product or selecting an optimal method of application.

Acknowledgements

This study has been partially supported by the projects: BIA2015-64878-R (Art-Risk, RETOS project of Ministerio de Economía y Competitividad and Fondo Europeo de Desarrollo Regional), CTQ2013-48396-P (Ministerio de Economía y Competitividad and Fondo Europeo de Desarrollo Regional) and the research teams TEP-199, P10-FQM-6615 and FQM-319 from Junta Andalucía. J. Becerra is grateful to the Ministerio de Educación, Cultura y Deporte for his pre-doctoral

fellowship (FPU14/05348) and to the University Ecclesiastical Academy of Thessaloniki for his stay as visiting researcher.

References

[1] Y. Nuhoglu, E. Oguz, H. Uslu, A. Ozbek, B. Ipekoglu, I. Ocak, I. Hasenekoglu, The accelerating effects of the microorganisms on biodeterioration of stone monuments under air pollution and continental-cold climatic conditions in Erzurum, Turkey, Sci. Total Environ. 364 (2006) 272–283. doi:10.1016/j.scitotenv.2005.06.034.

[2] M.E. Rabanal, R. Fort, New nanomaterials for applications in conservation and restoration of stony materials : A review, Mater. Construcción. 67 (2017). doi:10.3989/mc.2017.07616.

[3] A.M.M. Essa, M.K. Khallaf, Biological nanosilver particles for the protection of archaeological stones against microbial colonization, Int. Biodeterior. Biodegrad. 94 (2014) 31–37. doi:10.1016/j.ibiod.2014.06.015.

[4] R. Carrillo-González, M.A. Martínez-Gómez, M. del C.A. González-Chávez, J.C. Mendoza Hernández, Inhibition of microorganisms involved in deterioration of an archaeological site by silver nanoparticles produced by a green synthesis method, Sci. Total Environ. 565 (2015) 872–881. doi:10.1016/j.scitotenv.2016.02.110.

[5] P. Munafò, G.B. Goffredo, E. Quagliarini, TiO2-based nanocoatings for preserving architectural stone surfaces: An overview, Constr. Build. Mater. 84 (2015) 201–218. doi:10.1016/j.conbuildmat.2015.02.083.

[6] L. Graziani, E. Quagliarini, A. Osimani, L. Aquilanti, F. Clementi, C. Yéprémian, V. Lariccia, S. Amoroso, M. D'Orazio, Evaluation of inhibitory effect of TiO2 nanocoatings against microalgal growth on clay brick façades under weak UV exposure conditions, Build. Environ. 64 (2013) 38–45. doi:10.1016/j.buildenv.2013.03.003.

[7] I.D. van der Werf, N. Ditaranto, R.A. Picca, M.C. Sportelli, L. Sabbatini, Development of a novel conservation treatment of stone monuments with bioactive nanocomposites, Herit. Sci. 3 (2015) 29. doi:10.1186/s40494-015-0060-3.

[8] M. Rai, A. Yadav, A. Gade, Silver nanoparticles as a new generation of antimicrobials, Biotechnol. Adv. 27 (2009) 76–83. doi:10.1016/j.biotechadv.2008.09.002.

[9] J.S. Kim, E. Kuk, K.N. Yu, J.H. Kim, S.J. Park, H.J. Lee, S.H. Kim, Y.K. Park, Y.H. Park, C.Y. Hwang, Y.K. Kim, Y.S. Lee, D.H. Jeong, M.H. Cho, Antimicrobial effects of silver nanoparticles, Nanomedicine Nanotechnology, Biol. Med. 3 (2007) 95–101. doi:10.1016/j.nano.2006.12.001.

[10] F. Bellissima, M. Bonini, R. Giorgi, P. Baglioni, G. Barresi, G. Mastromei, B. Perito, Antibacterial activity of silver nanoparticles grafted on stone surface, Environ. Sci. Pollut. Res. 21 (2014) 13278–13286. doi:10.1007/s11356-013-2215-7.

[11] B. Gutarowska, J. Skora, K. Zduniak, D. Rembisz, Analysis of the sensitivity of microorganisms contaminating museums and archives to silver nanoparticles, Int. Biodeterior. Biodegrad. 68 (2012) 7–17. doi:10.1016/j.ibiod.2011.12.002.

[12] E. Quagliarini, F. Bondioli, G.B. Goffredo, C. Cordoni, P. Munafò, Self-cleaning and de-polluting stone surfaces: TiO2 nanoparticles for limestone, Constr. Build. Mater. 37 (2012) 51–57. doi:10.1016/j.conbuildmat.2012.07.006.

[13] M.F. La Russa, S.A. Ruffolo, N. Rovella, C.M. Belfiore, A.M. Palermo, M.T. Guzzi, G.M. Crisci, Multifunctional TiO2 coatings for Cultural Heritage, Prog. Org. Coatings. 74 (2012) 186–191. doi:10.1016/j.porgcoat.2011.12.008.

[14] H.A. Foster, I.B. Ditta, S. Varghese, A. Steele, Photocatalytic disinfection using titanium dioxide: Spectrum and mechanism of antimicrobial activity, Appl. Microbiol. Biotechnol. 90 (2011) 1847–1868. doi:10.1007/s00253-011-3213-7.

[15] J. Becerra, A.P. Zaderenko, M.J. Sayagués, R. Ortiz, P. Ortiz, Synergy achieved in silver-TiO2 nanocomposites for the inhibition of biofouling on limestone, Build. Environ. 141 (2018) 80–90. doi:10.1016/j.buildenv.2018.05.020.

[16] I. Yaşa, N. Lkhagvajav, M. Koizhaiganova, E. Çelik, Ö. Sari, Assessment of antimicrobial activity of nanosized Ag doped TiO2 colloids, World J. Microbiol. Biotechnol. 28 (2012) 2531–2539. doi:10.1007/s11274-012-1061-y.

[17] M. Lungu, Ş. Gavriliu, E. Enescu, I. Ion, A. Brătulescu, G. Mihăescu, L. Măruţescu, M.C. Chifiriuc, Silver-titanium dioxide nanocomposites as effective antimicrobial and antibiofilm agents, J. Nanoparticle Res. 16 (2014). doi:10.1007/s11051-013-2203-3.

[18] F.C. De Lucia, A.W. Miziolek, K.L. Mcnesby, R.A. Walters, P.D. French, Laser-induced breakdown spectroscopy (LIBS) – an emerging eld-portable sensor technology for real-

467 time, Sierra. (2005).

468 [19] D. Anglos, V. Detalle, Cultural Heritage Application of LIBS, in: Laser-Induced Break.
469 Spectrosc., 2014: pp. 531–554. doi:10.1007/978-3-642-45085-3.

470 [20] F. Colao, R. Fantoni, P. Ortiz, M.A.A. Vazquez, J.M.M. Martin, R. Ortiz, N. Idris, Quarry
471 identification of historical building materials by means of laser induced breakdown
472 spectroscopy, X-ray fluorescence and chemometric analysis, Spectrochim. Acta Part B At.
473 Spectrosc. 65 (2010) 688–694. doi:10.1016/j.sab.2010.05.005.

474 [21] S. Awasthi, R. Kumar, G.K. Rai, A.K. Rai, Study of archaeological coins of different
475 dynasties using libs coupled with multivariate analysis, Opt. Lasers Eng. 79 (2016) 29–38.
476 doi:10.1016/j.optlaseng.2015.11.005.

477 [22] L. Caneve, A. Diamanti, F. Grimaldi, G. Palleschi, V. Spizzichino, F. Valentini, Analysis of
478 fresco by laser induced breakdown spectroscopy, Spectrochim. Acta - Part B At.
479 Spectrosc. 65 (2010) 702–706. doi:10.1016/j.sab.2010.05.003.

480 [23] S. Guirado, F.J. Fortes, V. Lazic, J.J. Laserna, Chemical analysis of archeological materials
481 in submarine environments using laser-induced breakdown spectroscopy. On-site trials
482 in the Mediterranean Sea, Spectrochim. Acta - Part B At. Spectrosc. 74–75 (2012) 137–
483 143. doi:10.1016/j.sab.2012.06.032.

484 [24] S. Mahmood, S.A. Abbasi, S. Jabeen, M.A. Baig, Laser-induced breakdown spectroscopic
485 studies of marbles, J. Quant. Spectrosc. Radiat. Transf. 111 (2010) 689–695.
486 doi:10.1016/j.jqsrt.2009.11.012.

487 [25] P. Ortiz, V. Antúnez, R. Ortiz, J.M.M. Martín, M.A.A. Gómez, A.R.R. Hortal, B. Martínez-
488 Haya, Comparative study of pulsed laser cleaning applied to weathered marble surfaces,
489 Appl. Surf. Sci. 283 (2013) 193–201. doi:10.1016/j.apsusc.2013.06.081.

490 [26] P. Ortiz, V. Antunez, R. Ortiz, J.M. Ramírez, M.A. Gómez, M. Bethencourt, I. López, V.
491 Piñón, M.P. Mateo, G. Nicolás, IV Congreso Latinoamericano de Conservación y
492 Restauración de Metal, in: Grupo Español de Conservación (Ed.), IV Congr. Latinoam.
493 Conserv. y Restauración Met., Madrid, 2013: pp. 41–48.

494 [27] M.S. Rakotonirainy, L. Caillat, C. Héraud, J.B. Memet, Q.K. Tran, Effective biocide to
495 prevent microbiological contamination during PEG impregnation of wet archaeological
496 iron-wood artefacts, J. Cult. Herit. 8 (2007) 160–169. doi:10.1016/j.culher.2007.01.005.

[28] G. Borsoi, R. Van Hees, B. Lubelli, R. Veiga, A. Santos Silva, Nanolime deposition in Maastricht limestone : back-migration or accumulation at the absorption surface?, in: EMABM 2015 Proc. 15th Euroseminar Microsc. Appl. to Build. Mater. Delft, Netherlands, 17-19 June 2015, Delft University of Technology, Delft, 2015: pp. 77–86.

[29] F. Gherardi, A. Colombo, M. D'Arienzo, B. Di Credico, S. Goidanich, F. Morazzoni, R. Simonutti, L. Toniolo, Efficient self-cleaning treatments for built heritage based on highly photo-active and well-dispersible TiO2 nanocrystals, Microchem. J. 126 (2016) 54–62. doi:10.1016/j.microc.2015.11.043.

[30] P. Ortiz, M.A. Guerrero, M.A. Vázquez;, R. Ortiz;, J.M. Martin;, M.C.C. Peña, Accelerated weathering test as environmental behaviour trials on calcareous stone, in: Proc. XIth Int. Congr. Deterior. Conserv. Stone. I., Polonia, 2008: pp. 223–232.

[31] R. Fort, A. Bernabéu, M.A. García del Cura, M.C. López de Azcona, S. Ordóñez, F. Mingarro, Novelda Stone: widely used within the Spanish architectural heritage, Mater. Construcción. 52 (2002) 19–32. doi:10.3989/mc.2002.v52.i266.332.

[32] M.A. Bello, A. Martín, Microchemical Characterization of Building Stone From Seville Cathedral, Spain, Archaeometry. 34 (1992) 21–29. doi:10.1111/j.1475-4754.1992.tb00473.x.

[33] M.A. Guerrero, Diagnóstico del estado de alteración de la piedra del Palacio Consistorial de Sevilla. Causas y mecanismos, Universidad de Sevilla (Spain), 1990.

[34] Asociación Española de Normalización y Certificación, UNE-EN 13755: Natural stone test methods. Determination of water absorption at atmospheric pressure., 2008.

[35] L. Pinho, M. Rojas, M.J. Mosquera, Ag–SiO2–TiO2 nanocomposite coatings with enhanced photoactivity for self-cleaning application on building materials, Appl. Catal. B Environ. 178 (2015) 144–154. doi:10.1016/j.apcatb.2014.10.002.

[36] P. Sanmartín, F. Villa, A. Polo, B. Silva, B. Prieto, F. Cappitelli, Rapid evaluation of three biocide treatments against the cyanobacterium Nostoc sp. PCC 9104 by color changes, Ann. Microbiol. 65 (2015) 1153–1158. doi:10.1007/s13213-014-0882-3.

[37] L. Graziani, E. Quagliarini, M. D'Orazio, The role of roughness and porosity on the self-cleaning and anti-biofouling efficiency of TiO2-Cu and TiO2-Ag nanocoatings applied on fired bricks, Constr. Build. Mater. 129 (2016) 116–124.

527 doi:10.1016/j.conbuildmat.2016.10.111.

528 [38] O. García, K. Malaga, Definition of the procedure to determine the suitability and
529 durability of an anti-graffiti product for application on cultural heritage porous materials,
530 J. Cult. Herit. 13 (2012) 77–82. doi:10.1016/j.culher.2011.07.004.

531 [39] B. Prieto, B. Silva, O. Lantes, Biofilm quantification on stone surfaces: Comparison of
532 various methods, Sci. Total Environ. 333 (2004) 1–7.
533 doi:10.1016/j.scitotenv.2004.05.003.

534 [40] W. De Muynck, A.M. Ramirez, N. De Belie, W. Verstraete, Evaluation of strategies to
535 prevent algal fouling on white architectural and cellular concrete, Int. Biodeterior.
536 Biodegrad. 63 (2009) 679–689. doi:10.1016/j.ibiod.2009.04.007.

537 [41] P. Sanmartín, D. Vázquez-Nion, B. Silva, B. Prieto, Spectrophotometric color
538 measurement for early detection and monitoring of greening on granite buildings.,
539 Biofouling. 28 (2012) 329–38. doi:10.1080/08927014.2012.673220.

540 [42] P. Sanmartín, F. Villa, B. Silva, F. Cappitelli, B. Prieto, Color measurements as a reliable
541 method for estimating chlorophyll degradation to phaeopigments, Biodegradation. 22
542 (2011) 763–771. doi:10.1007/s10532-010-9402-8.

543 [43] D.C. Smith, C. Carabatos-Nedel, Raman Spectroscopy Applied to Crystals: Phenomena
544 and Principles, Concepts and Conventions, in: I.R. Lewis, H. l G.M. Edwards (Eds.), Handb.
545 Raman Spectrosc. From Res. Lab. to Process Line, Marcel Dekker, Inc., New-York, Basel,
546 2001: pp. 349–422.

547 [44] N. Biswas, S. Kapoor, H.S. Mahal, T. Mukherjee, Adsorption of CGA on colloidal silver
548 particles: DFT and SERS study, Chem. Phys. Lett. 444 (2007) 338–345.
549 doi:10.1016/j.cplett.2007.07.049.

550 [45] A. Kora, S. Beedu, A. Jayaraman, Size-controlled green synthesis of silver nanoparticles
551 mediated by gum ghatti (Anogeissus latifolia) and its biological activity, Org. Med. Chem.
552 Lett. 2 (2012) 17. doi:10.1186/2191-2858-2-17.

553 [46] W.F. Zhang, Y.L. He, M.S. Zhang, Z. Yin, Q. Chen, Raman scattering study on anatase
554 TiO2nanocrystals, J Phys D Appl Phys. 33 (2000). doi:10.1088/0022-3727/33/8/305.

555 [47] P.K. Koutsoukos, P.G. Klepetsanis, N. Spanos, Calculation of Zeta-Potentials from
556 Electrokinetic Data, in: P. Somasundaran (Ed.), Encycl. Surf. Colloid Sci., Taylor & Francis

557 Group, New York, 2006: pp. 1097–1113. doi:10.1081/E-ESCS-120000059.

558 [48] S. Kapoor, Preparation , Characterization , and Surface Modification of Silver Particles,
559 Langmuir. 14 (1998) 1021–1025.

560 [49] J. Becerra, A.P. Zaderenko, P. Ortiz, A.P.Z. Partida, P.O. Calderón, Silver/dioxide titanium
561 nanocomposites as biocidal treatments on limestones, Ge-Conservación. 11 (2017) 141–
562 148.

563 [50] A.J. Fonseca, F. Pina, M.F. Macedo, N. Leal, A. Romanowska-Deskins, L. Laiz, A. Gómez-
564 Bolea, C. Saiz-Jimenez, Anatase as an alternative application for preventing
565 biodeterioration of mortars: Evaluation and comparison with other biocides, Int.
566 Biodeterior. Biodegrad. 64 (2010) 388–396. doi:10.1016/j.ibiod.2010.04.006.

567